

# On the characteristics of tidal structures of interacting galaxies

Y.H. Mohamed<sup>1,2</sup>, V.P. Reshetnikov<sup>1</sup>, N.Ya. Sotnikova<sup>1</sup>

<sup>1</sup> St.Petersburg State University, Universitetskii pr. 28, Petrodvoretz, 198504 Russia

<sup>2</sup> Astronomy Department, National Research Institute of Astronomy and Geophysics, Cairo 11421, Egypt

We present the results of our analysis of the geometrical tidal tail characteristics for nearby and distant interacting galaxies. The sample includes more than two hundred nearby galaxies and about seven hundred distant ones. The distant galaxies have been selected in several deep fields of the Hubble Space Telescope (HDF-N, HDF-S, HUDF, GOODS, GEMS) and they are at mean redshift  $\langle z \rangle = 0.65$ . We analyze the distributions of lengths and thicknesses for the tidal structures and show that the tails in distant galaxies are shorter than those in nearby ones. This effect can be partly attributed to observational selection effects, but, on the other hand, it may result from the general evolution of the sizes of spiral galaxies with  $z$ . The location of interacting galaxies on the galaxy luminosity ( $L$ ) – tidal tail length ( $l$ ) plane are shown to be explained by a simple geometrical model, with the upper envelope of the observed distribution being  $l \propto \sqrt{L}$ . We have solved the problem on the relationship between the observed distribution of tail flattening and the tail length in angular measure by assuming the tidal tails to be arcs of circumferences visible at arbitrary angles to the line of sight. We conclude that the angular length of the tidal tails visually distinguished in nearby and distant galaxies, on average, exceeds  $180^\circ$ .

**Keywords:** galaxies, interacting galaxies, morphology, kinematics.

## 1. Introduction

Tidal structures (the tails and the bridges connecting galaxies) are transient features emerging during close encounters and mergers of galaxies (Toomre and Toomre 1972). As a rule, tidal structures have a low optical surface brightness ( $\mu(B) \approx 24^m - 25^m / \square''$ ) and they are observed in several percent of galaxies in the local Universe (for an overview, see Sotnikova and Reshetnikov 1998a; Reshetnikov and Sotnikova 2001).

Tidal structures are interesting for many reasons. For example, dwarf galaxies can be formed from their matter (Duc 2011). The formation of massive clumps, up to  $10^8 M_\odot$ , by the gravitational collapse of stars and gas clouds extended into the tidal tail are commonly observed in numerical simulations of galaxy interactions (see, e.g., Barnes and Hernquist 1992; Elmegreen et al. 1993). Such clumps can give rise to dwarf galaxies.

The current star formation rate in tidal tails is occasionally high; the star-forming regions (HII regions) can be arranged in the tail uniformly, as, for example,

in the tail of NGC 4676 A (Sotnikova and Reshetnikov 1998b). In the discs of normal galaxies, star formation usually takes place in giant  $H_2$  complexes. Tidal structures are formed from the diffuse gas stretched from the outermost regions of a galaxy. The question about the star formation mechanism in these structures is open. For example, such a mechanism may be associated with global gravitational instability in tails (Sotnikova and Reshetnikov 1998b).

The morphology of tails and bridges is determined by the global dynamical structure of galaxies. For example, it has emerged that the length of tidal tails depends not only on the impact parameters and the relative velocity of interacting galaxies but also on the mass distribution of dark matter (see, e.g., Dubinski et al. 1996, 1999; Mihos et al. 1998; Springel and White 1999). Having analyzed the results of numerical simulations, Dubinski et al. (1996) noticed that if the mass of dark matter is large enough, then the forming tidal tails turn out to be too short and indistinct. At the same time, in interacting and merging

systems, we often observe very extended tidal structures stretching to distances as large as 50–100 kpc.

The conclusion that extended tidal tails can serve as an indicator for the presence of dark matter in the outermost regions of galaxies, where the HI disc is invisible, is also corroborated by kinematic data. Using the primary component of the famous interacting system NGC 4676 (the Mice) as an example, Sotnikova and Reshetnikov (1998b) concluded that the kinematics of the tidal tail (its length exceeds 40 kpc) is consistent only with the model of a dark halo whose mass within the optical tail exceeds the total mass of the galactic disc and bulge by several times.

Mutual agreement between the kinematic and morphological analyses suggests that conclusions about dark halo characteristics can be made even though the spectroscopic data are not available and we have only photometric data (in the case of distant galaxies with tidal features having a low surface brightness).

The occurrence of tidal structures at different redshifts is of great interest, because it reflects the change in the rate of galaxy mergers and interactions with time (Reshetnikov 2000; Bridge et al. 2010).

The main goal of this paper is to study basic geometrical characteristics of the tidal tails in several hundred nearby and distant interacting galaxies so as to reach conclusions about the relationship between these characteristics and the global parameters of the galaxies themselves. All numerical values in the paper are given for the cosmological model with a Hubble constant of  $70 \text{ km s}^{-1} \text{ Mpc}^{-1}$  and  $\Omega_m = 0.3$ ,  $\Omega_\Lambda = 0.7$ .

## 2. The samples of galaxies and the measured parameters

### 2.1. Nearby and distant galaxies with tidal structures

To study the characteristics of nearby galaxies, we considered two samples: (1) KPG – binary galaxies from the catalog by Karachentsev (1987); (2) SDSS – galaxies with tidal tails from the catalog by Nair and Abraham (2010) based on the visual classification of 14 034 objects from the Sloan Digital Sky Survey. The first sample includes 44 galaxies for which the characteristics of their tidal structures could be measured in the Digital Sky Survey (DSS); the second sample includes 182 objects with tidal structures clearly distinguishable in the SDSS. Since many of the galaxies studied exhibit not one but two tails, the number of tidal tails we measured (64 and 266 in the KPG and

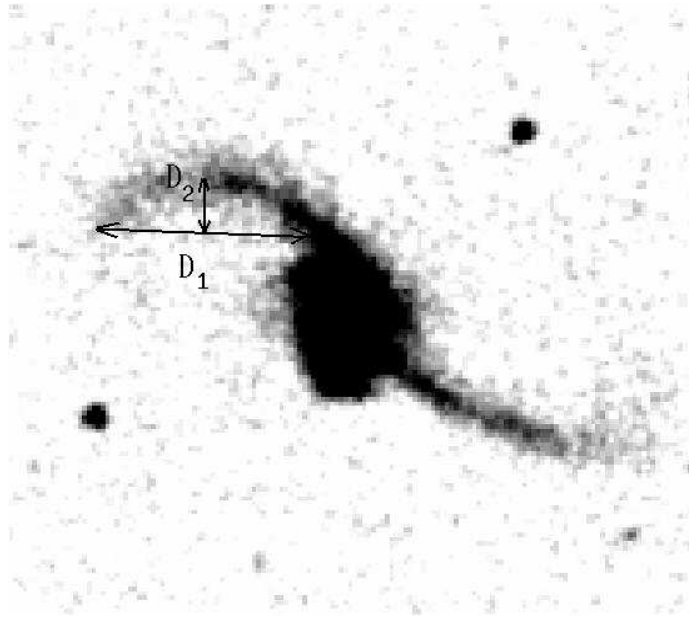


**Fig. 1.** Determining  $D_1$  and  $D_2$  for tidal tails using a high-contrast DSS image of the nearby merging system NGC 2623 as an example:  $D_1$  is the length of the segment connecting the beginning and the end of the tidal structure,  $D_2$  is the size of the perpendicular drawn from the center of this segment to the tail.

SDSS samples, respectively) exceeds the number of galaxies.

When studying distant galaxies, we used the catalog of interacting galaxies found in deep fields of the Hubble Space Telescope (Mohamed and Reshetnikov 2011). This catalog includes data for about seven hundred candidates for galaxies with tidal structures ( $z \leq 1.5$ ) in several Hubble deep fields (HDF-N, HDF-S, HUDF, GOODS, GEMS). The investigated fields partly overlap (e.g., HUDF is part of GOODS) and, in these cases, the characteristics of galaxies were estimated from the deeper field. We studied a total of 867 tidal structures in all deep fields.

### 2.2. Parameters of tidal structures

For all interacting galaxies, we determined the geometrical characteristics of their tidal structures from high-contrast optical images: the length of the tail from the edge of the galactic disc to its end ( $l$ ) measured along the curved tail, the half-length width ( $h$ ), and the ratio  $k = D_2/D_1$ , which is a measure of the curvature (see Fig. 1). It is obvious that  $k = 0$  for a straight tail and  $k > 0$  for a curved one. If the tail is assumed to be an arc of a circumference, then  $k$  for an arc of  $180^\circ$  is equal to 0.5. (All the measure-

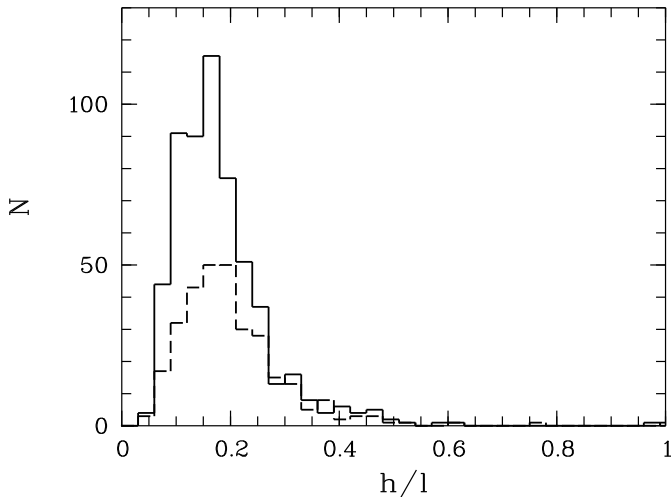


**Fig. 2.** The distributions of relative tail thicknesses ( $h/l$ ) for nearby (dashed line) and distant (solid line) galaxies with  $l \geq 10$  kpc.

ment were done within the surface brightness limit of  $\mu(I) \approx 25 - 26$ .)

When analyzing the objects from the KPG sample, we used blue DSS images; for the objects from Nair and Abraham (2010), we took data in the  $g$  band ( $\lambda_{eff} = 4686 \text{ \AA}$ ). The characteristics of galaxies from the deep fields were determined in the F814W (HDF-N, HDF-S), F775W (HUDF), and F850LP (GOODS and GEMS) filters (at redshift  $z \sim 1$ ) these filters roughly correspond to the  $B$  band in the reference frame associated with the galaxy). To verify the nature of the tidal structures in faint distant galaxies, we performed their aperture photometry at several points along the structures. The mean surface brightness of the tails recalculated to the  $B$  band in the reference frame associated with the galaxy ( $\langle \mu_B \rangle = 24.7 \pm 1.1(\sigma)$ ) turned out to be close to its typical values for the tidal structures of local galaxies (see, e.g., Schombert et al. 1990; Reshetnikov 1998).

The redshift estimates and apparent magnitudes are available for all of the distant galaxies we considered (Fernandez-Soto et al. 1999; Williams et al. 2000; Sawicki and Mallen-Ornelas 2003; Wolf et al. 2004; Glazebrook et al. 2006; Coe et al. 2006; Balestra et al. 2010), allowing to find the galaxy luminosities. The mean redshift of our sample of distant interacting galaxies is  $\langle z \rangle = 0.65 \pm 0.31(\sigma)$ .

### 3. Results and discussion

#### 3.1. Geometrical characteristics of tidal tails

Figure 2 shows the observed distributions of thicknesses for the tidal structures in nearby and distant galaxies with relatively long ( $l \geq 10$  kpc) tails. Both distributions are similar and they demonstrate peaks of observed flattening at  $h/l \approx 0.15$ . As we see from the figure, there are very thin ( $h/l \leq 0.1$ ) and relatively wide ( $h/l \geq 0.2$ ) tails.

Figure 3a shows the distributions of tail lengths in the KPG and SDSS samples of nearby galaxies. The distributions are similar and they exhibit global maxima at  $l \approx 20$  kpc. Figure 3b displays the analogous distribution for distant galaxies in comparison with the combined (KPG + SDSS) distribution for nearby ones. In this figure, we see the difference between the two distributions: for distant galaxies, the maximum occurs at  $l \approx 10$  kpc. Moreover, among the most distant galaxies, extended ( $l > 30$  kpc) tidal structures are less common. It is somewhat premature to conclude about the evolution of the tail lengths with  $z$ , because the statistics of the lengths of tidal structures for distant galaxies is undoubtedly distorted by observational selection. The most important selection effects, that lead a rapid decrease in brightness, are the cosmological surface brightness dimming (Tolman's effect) and the  $k$  correction. When measuring the tail lengths within a fixed isophote, we will obtain systematically progressively shorter structures as the redshift increases.

To avoid these effects, at least partially, we measured the tail length in diameters of the galaxy's main body ( $d$ ). The diameter was estimated simultaneously with the tail length and it corresponds to approximately the same brightness level. Since the cosmological dimming and the  $k$  correction must reduce the measured angular size of a galaxy, the ratio of the tail length to the diameter of the main galaxy is affected by these effects to a lesser extent. Figure 3c shows the observed distributions of relative tail lengths for the samples of nearby galaxies. These distributions are similar and they exhibit peaks at  $l/d \approx 1.5 - 2$ . Figure 3d displays the distribution of relative tail lengths for distant galaxies in comparison with the combined distribution for nearby ones. We see from this figure that there is no statistically significant difference between the two distributions: the relative length of the tidal tails in distant galaxies, just as in nearby ones, exhibits a maximum at  $l/d \approx 1.5 - 2$  (the corresponding median values are 1.99 and 1.80).

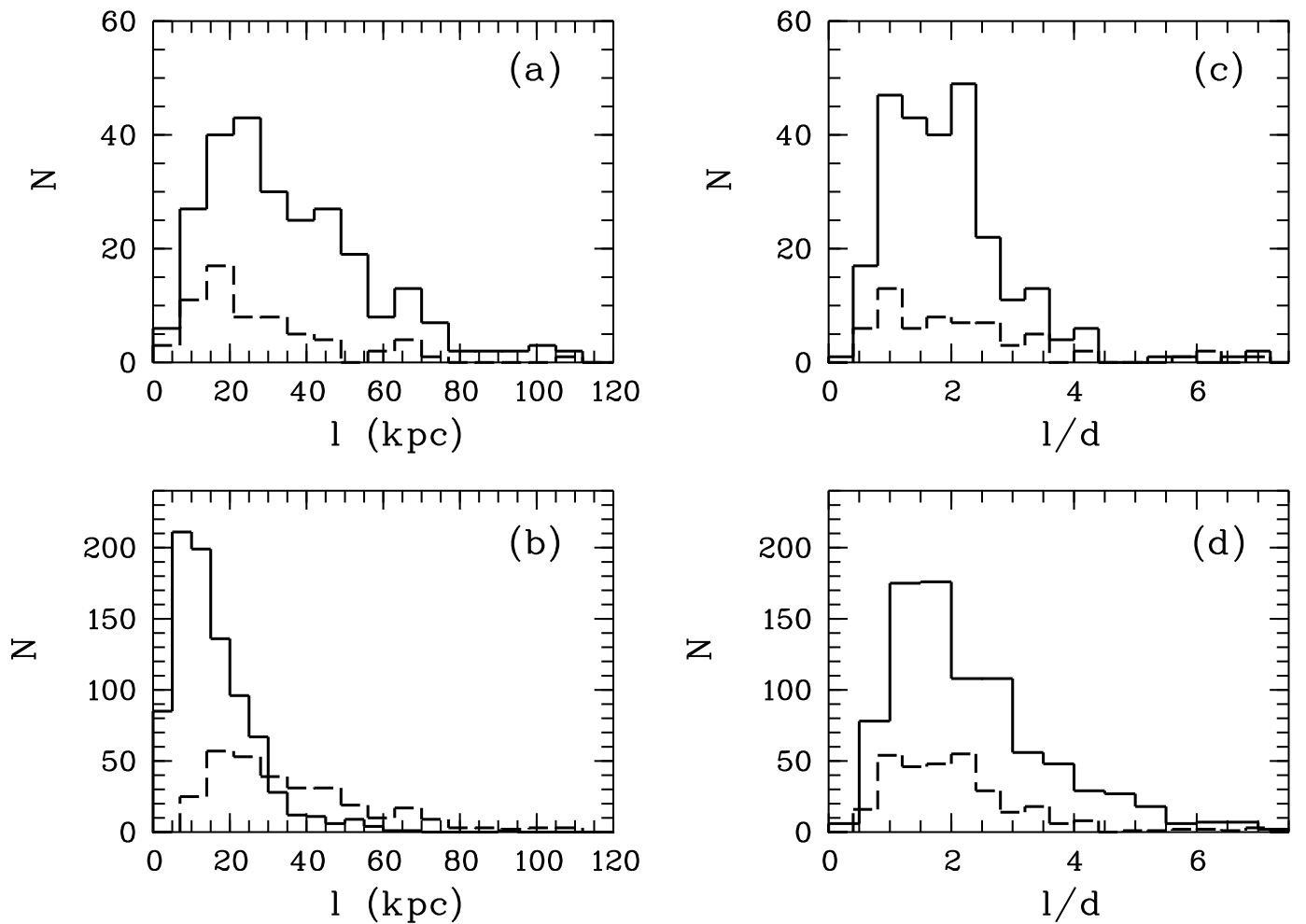


**Fig. 3.** The distributions of absolute (a, b) and relative (c, d) tidal tail lengths for nearby and distant galaxies: (a) the solid and dashed lines indicate the distributions of tail lengths for the nearby galaxies from the SDSS and KPG samples, respectively; (b) the distant and nearby (the combined KPG + SDSS sample) objects are indicated by the solid and dashed lines, respectively; (c) the relative tail lengths ( $l/d$ ) in the SDSS (solid line) and KPG (dashed line) samples; (d) the distributions of distant (solid line) and nearby (KPG + SDSS) galaxies in  $l/d$ .

The relationships between the relative ( $l/d$ ) and linear tail lengths for nearby and distant galaxies shown in Fig. 4 differ noticeably. Previously, Elmegreen et al. (2007) considered the  $l/d-l$  plane for about twenty distant (from the GEMS and GOODS fields) and nearby galaxies with extended tidal structures. They found the tails of nearby galaxies to be a factor of 2.7 longer than those of distant ones. Our data confirm this result: as we see from Fig. 4, the tails of nearby galaxies at fixed  $l/d$  are appreciably

(on average, by a factor of 2.6) longer. Such a good quantitative agreement between the results obtained from samples differing by several tens of times is remarkable, although it may be partly accidental.

The observed difference between the linear lengths of tidal structures can be attributed, at least partly, to observational selection. On the other hand, it can reflect the actually observed evolution of the sizes of spiral galaxies and, as a consequence, the sizes

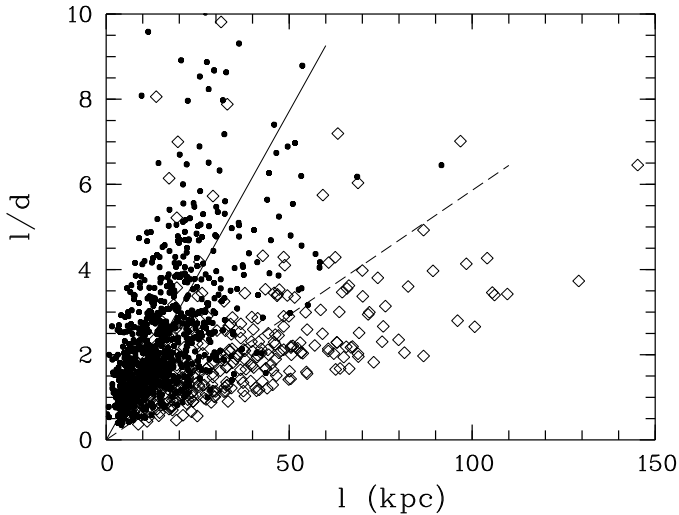


**Fig. 4.** Nearby (diamonds) and distant (filled circles) galaxies on the  $l - l/d$  plane. The linear regression is indicated by the solid and dashed straight lines for distant and nearby galaxies, respectively. In order to reconcile the slopes of these dependencies, tail lengths for distant galaxies should be increased by a factor of 2.6.

of their tidal structures (for a discussion, see the Conclusions).

### 3.2. The galaxy luminosity – tail length relationship

The relationship between the absolute magnitude of a galaxy and the length of its tidal tail is shown in Fig. 5. This relationship can indirectly reflect the connection between the length of tails and the global dynamical structure of galaxies expected from theoretical considerations (Dubinski et al. 1996, 1999; Mihos et al. 1998; Springel and White 1999).

The formation of a tidal tail is a purely energetic effect. The disc stars must acquire the energy sufficient to escape out to a distance equal to the tail length. The energy acquisition depends on two competing factors: the galaxy interaction time and the strength of perturbation. Both depend on the mass distribution, primarily in the dark halo, or on the potential gradient. Bright galaxies probably possess, on average, massive dark halos. In this case, the action of the perturbing force will be more likely impulsive than resonant. This implies that such galaxies will form less extended tails during their interaction.

Another difficulty arises in the case of low-mass dark halos. Although the tidal tails turn out to be

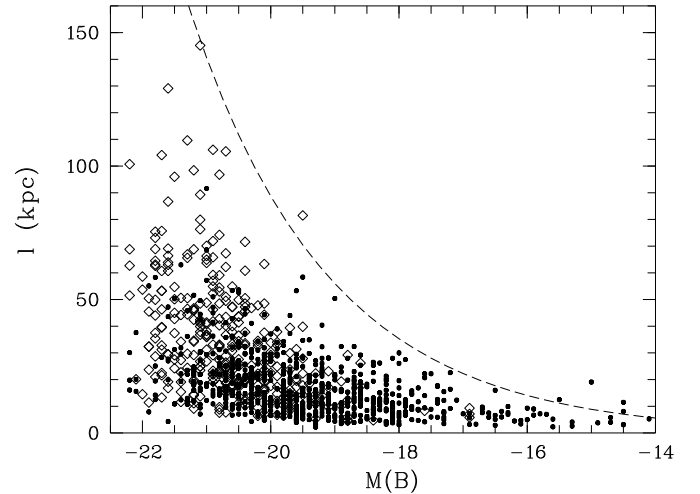


**Fig. 5.** Total galaxy luminosity versus tail length. The data for nearby and distant galaxies are indicated by the diamonds and filled circles, respectively. The dashed line indicates the dependence  $l \propto \sqrt{L}$  following from simple geometrical considerations (see the text).

very long, the interacting galaxies merge very rapidly. That is why the relation between the dark halo mass and the tidal tail length is ambiguous. It should also be noted that the length of the tidal tail depends strongly not only on the depth of the potential well but also on the initial distribution of visible matter (stars and gas) in the disk of the parent galaxy (Sotnikova and Reshetnikov 1998b). If, for example, the tidal tails are assumed to be formed mainly from gas in which a starburst subsequently occurs, then extended features can be obtained in models with large dark halo mass.

Thus, it is rather difficult to construct an unambiguous relation between the tidal tail length and the dark halo mass that can be associated with the total galaxy luminosity. It is much easier to try to find the direct relationship between the galaxy luminosity and the tidal tail length suggesting a simple model.

Let us consider the following geometrical model. We suppose that a fixed fraction of the galactic mass goes into the galaxy's tidal tail and that this matter has the same mass-to-light ratio as that of the galaxy itself. The surface brightness of the tail will then be determined by its luminosity divided by the area that in our notation is equal to  $\beta \times l^2$ , where  $\beta = h/l$ . At fixed surface brightness and relative width of the tail, we can then immediately obtain the relation between

the total galaxy luminosity and the tail length. In the  $B$  band, this relation is

$$\lg l = -0.2(M_{\text{tot}} + \alpha) - 0.5 \lg \beta + 0.2 \mu_{\text{tail}} - 7.31, \quad (1)$$

where the tail length  $l$  is in kpc,  $M_{\text{tot}}$  is the absolute magnitude of the galaxy,  $\alpha$  is the difference between the absolute magnitude of the tail and the galaxy (for example, if the tail luminosity is 10% of the total galaxy luminosity, then  $\alpha = 2.^m5$ ),  $\beta$  is the relative width of the tail, and  $\mu_{\text{tail}}$  is its surface brightness.

The dashed line in Fig. 5 indicates dependence (1) (it is  $l \propto \sqrt{L}$ , where  $L$  is the total luminosity of the galaxy) for the following parameters:  $\alpha = 1.^m75$ , i.e. the luminosity of the tidal structure is 20% of the total luminosity,  $\beta = 0.15$  and  $\mu_{\text{tail}} = 26^m/\square''$ . Wider, brighter, and relatively less luminous tails must lie under this model dependence. As we see from the figure, the simple geometrical model describes satisfactorily the upper envelope of the actual distribution of galaxies. This implies that the visually distinguished optical tidal tails constitute a relatively homogeneous class of objects that can be characterized, on average, by a fixed fraction of the luminosity of the main galaxy and by typical thickness and surface brightness values.

### 3.3. The length of tidal tails in angular measure

It is difficult to determine the shape of the tidal tails that often have an intricate pattern in projection. As the first approximation, we assumed the tails to be arcs of circumferences visible at arbitrary angles to the line of sight. In this case, the observed distribution of apparent flattenings of the arcs, characterized by the parameter  $k$  that we introduced above, will depend on the angular measure of the arcs.

Consider the simplest model. Let us take a circumference of unit radius oriented arbitrarily in space. Let us choose an arbitrary arc of fixed angular length  $\Delta\varphi$ . In projection onto the plane of the sky, the circumference will appear as an ellipse with an axial ratio  $b/a = \cos i$ , where  $i$  is the inclination of the circumference to the plane of the sky. The arc chosen on the circumference in projection will transform into an ellipse arc. For the projection of the circumference arc onto the plane of the sky, we can find the distance between the extreme points of the arc  $D_{1,\text{mod}}$  and the curvature of the ‘‘elliptic’’ arc  $D_{2,\text{mod}}$  as the distance between the straight line connecting the extreme points of the arc and the tangent to the arc running parallel to the first straight line.

In the plane of the sky, we will introduce a coordinate system in such a way that the  $x$  axis will coincide with the line of nodes (the line along which the circumference intersects with the plane of the sky) and the  $z$  axis will coincide with the line of sight. In the plane in which the circumference lies, we will also direct the  $x'$  axis along the line of nodes. The angle between the  $y$  and  $y'$  axes, just as between the  $z$  and  $z'$  axes, will then be equal to  $i$ .

Let us choose an arc on the circumference. We will denote the coordinates of its ends by  $(x'_1, y'_1) = (\cos \varphi_1, \sin \varphi_1)$  and  $(x'_2, y'_2) = (\cos(\varphi_1 + \Delta\varphi), \sin(\varphi_1 + \Delta\varphi))$ , where  $\varphi_1$  is the angle in the circumference plane measured from the line of nodes to the initial end of the arc and  $\Delta\varphi$  is the arclength. The coordinates of the ends of the arc projected onto the plane of the sky will then be  $(x_1, y_1) = (\cos \varphi_1, \sin \varphi_1 \cos i)$  and  $(x_2, y_2) = (\cos(\varphi_1 + \Delta\varphi), \sin(\varphi_1 + \Delta\varphi) \cos i)$ . From very simple geometrical considerations, we can obtain the following expression for the distance between the ends of the projected arc:

$$D_{1,\text{mod}}^2 = 4 \sin^2 \frac{\Delta\varphi}{2} \left[ 1 - \cos^2 \left( \varphi_1 + \frac{\Delta\varphi}{2} \right) \sin^2 i \right]. \quad (2)$$

The curvature of the arc can be expressed from the same geometrical considerations as

$$D_{2,\text{mod}}^2 = \frac{\left( 1 - \sin \frac{\Delta\varphi}{2} \right)^2 \cos^2 i}{1 - \cos^2 \left( \varphi_1 + \frac{\Delta\varphi}{2} \right) \sin^2 i}. \quad (3)$$

We will write the parameter characterizing the flattening of the projected arc,  $k_{\text{mod}} = D_{2,\text{mod}}/D_{1,\text{mod}}$ , as

$$k_{\text{mod}} = \frac{1}{2} \text{tg} \left( \frac{\Delta\varphi}{4} \right) \frac{\cos i}{1 - \cos^2 \left( \varphi_1 + \frac{\Delta\varphi}{2} \right) \sin^2 i}. \quad (4)$$

The distribution function of the angle  $i$  between the fixed plane (the plane of the sky) and an arbitrary plane is  $f(i) di = \sin i di$ , where  $i \in [0, \pi/2]$  (Agekyan 1974). The angle  $\varphi_1$  randomly runs the values from 0 to  $2\pi$ .

We randomly generated the values of  $i$  and  $\varphi_1$  in accordance with their distribution functions, determined  $k_{\text{mod}}$  for each realization at fixed  $\Delta\varphi$  and constructed the distribution of  $k_{\text{mod}}$ . Figure 6 reproduces this distribution for several values of  $\Delta\varphi$ . The distributions have a maximum near

$$k_{\text{mod}}^{\text{max}} = \frac{1}{2} \text{tg} \left( \frac{\Delta\varphi}{4} \right).$$

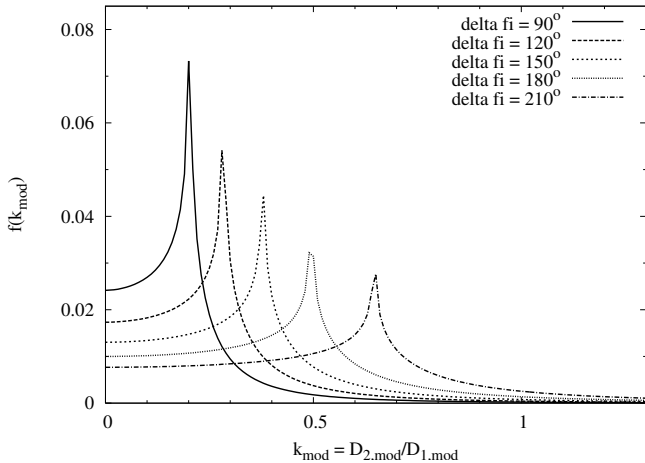


**Fig. 6.** The distribution of  $k_{\text{mod}} = D_{2,\text{mod}}/D_{1,\text{mod}}$ , characterizing the curvature of the projection of the circumference arc onto the plane of the sky for various arc lengths in angular measure  $\Delta\varphi$ .

Such a curvature of the arc is obtained when  $i = 0$ . In this case, any arbitrary segment of the circumference arc of fixed angular measure  $\Delta\varphi$  will give the same value of  $k_{\text{mod}}$ , which is responsible for the existence of the maximum  $k_{\text{mod}}^{\text{max}}$ .

The second prominent feature is the presence of a long plateau in the range of small  $k_{\text{mod}}$ . The arc is seen as an almost straight line if it is observed at an angle  $i$  close to  $90^\circ$ . In this case, the values of  $k_{\text{mod}}$  will be very low virtually irrespective of the choice  $\varphi_1$  (the initial point of the arc on the circumference) and the total contribution from these projections to the distribution function will remain at a fairly high level, producing an extended plateau.

The observed distribution of  $k$  is shown in Fig. 7a. We see that here there is no such sharp maximum as that observed for the model distributions. However, the position of the maximum indicates that the arcs with angular size  $> 180^\circ$  mainly contribute to the distribution of  $k$ .

We generated a model distribution of  $k_{\text{mod}}$  for arcs for which the length  $\Delta\varphi$  was not strictly fixed but had a scatter  $\sigma$  around its mean value ( $\Delta\varphi$ ) in accordance with the normal distribution. The model distributions are shown in Fig. 7b. The data in the figure confirm our conclusion that, if the tidal tails are assumed to be arcs of a circumference, then their angular length is, on average, greater than 180 degrees, i.e., they wind around the disks of galaxies by more than one half turn.

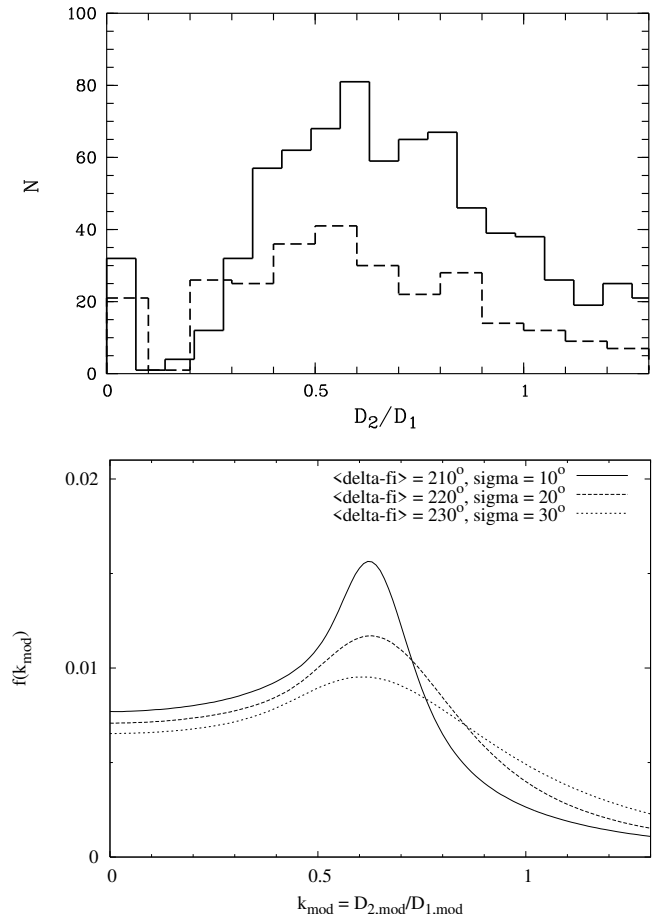


**Fig. 7.** Top: The distributions of nearby (dashed line) and distant (solid line) galaxies in  $k = D_2/D_1$ . Bottom: The model distribution of  $k_{\text{mod}} = D_{2,\text{mod}}/D_{1,\text{mod}}$  characterizing the curvature of the projection of the circumference arc onto the plane of the sky under the assumption that the arc length in angular measure  $\Delta\varphi$  is distributed normally.

#### 4. Conclusions

We investigated the geometrical characteristics of the tidal tails in large samples of nearby and distant interacting galaxies. It turned out that the visually distinguished tidal structures, on average, constitute a homogeneous class of objects that can be characterized by typical linear and angular lengths, surface brightness, and total luminosity at a given galaxy luminosity. Of course, this conclusion refers only to optically emitting structures, i.e., those containing a considerable number of stars, that are relatively easily discernible in digital surveys.

The observed tail length for distant galaxies turned out to be, on average, smaller than that for nearby ones. This is probably due to the combination of selection effects and the actual evolution of galaxy

properties. The cosmological dimming and the influence of the  $k$  correction can be attributed to the selection effects, as a result of which we observe only the brightest regions of tidal structures in distant objects. In addition, as a possible result of the decline in brightness with  $z$ , in distant galaxies we predominantly observe a relatively early evolutionary stage of the tails ( $\sim 10^8$  yrs at  $z = 1$ , see Mihos 1995), when they are still relatively bright and short, while in nearby objects we see, on average, “older” ( $\sim 10^9$  yrs) and longer structures.

On the other hand, present-day observations and models of the evolution of galaxies show that compared to their current characteristics, the spiral galaxies at  $z \sim 0.5 - 1$  must have been a factor 1.5–2 smaller in size and less massive by approximately the same factor (see, e.g., Dutton et al. 2011). This may imply that at the evolutionary phase of tidal structures when we predominantly recognize them by visually analyzing the images of galaxies, i.e., when their linear length is comparable to the size of the main galaxy (see Fig. 3) and the angular length reaches  $\geq 180^\circ$  (Fig. 7), they will be, on average, shorter than those in nearby objects.

The reasons noted above make it much more difficult to use the statistics of the lengths of tidal tails for galaxies at various  $z$  to study the properties of their dark halos. Only a detailed simulation of specific interacting systems can probably help establish well-defined relationships between the tail lengths and the dynamical properties of galaxies at various redshifts.

## Acknowledgments

This work was supported by the Russian Foundation for Basic Research (project no. 11-02-00471).

## REFERENCES

1. T.A. Agekyan, *Probability Theory for Astronomers and Physicists* (Nauka, Moscow, 1974) [in Russian].
2. I. Balestra, V. Mainieri, P. Popesso, et al., *Astron. Astrophys.* 512, 12 (2010).
3. J. Barnes and L. Hernquist, *Nature* 360, 715 (1992).
4. C.R. Bridge, R.G. Carlberg, and M. Sullivan, *Astrophys. J.* 709, 1067 (2010).
5. D. Coe, N. Benitez, S.F. Sanchez, et al., *Astron. J.* 132, 926 (2006).
6. J. Dubinski, J.Ch. Mihos, and L. Hernquist, *Astrophys. J.* 462, 576 (1996).
7. J. Dubinski, J.Ch. Mihos, and L. Hernquist, *Astrophys. J.* 526, 607 (1999).
8. P.-A. Duc, arXiv:1101.4834v2 (2011).
9. A.A. Dutton, F.C. van den Bosch, S.M. Faber, et al., *Mon. Not. R. Astron. Soc.* 410, 1660 (2011).
10. B.G. Elmegreen, M. Kaufman, and M. Thomasson, *Astrophys. J.* 412, 90 (1993).
11. D.M. Elmegreen, B.G. Elmegreen, Th. Ferguson, and B. Mullan, *Astrophys. J.* 663, 734 (2007).
12. A. Fernandez-Soto, K.M. Lanzetta, and A. Yahil, *Astrophys. J.* 513, 34 (1999).
13. K. Glazebrook, A. Verma, B. Boyle, et al., *Astron. J.* 131, 2383 (2006).
14. I.D. Karachentsev, *Binary Galaxies* (Nauka, Moscow, 1987) [in Russian].
15. J.Ch. Mihos, *Astrophys. J.* 438, L75 (1995).
16. J.Ch. Mihos, J. Dubinski, and L. Hernquist, *Astrophys. J.* 494, 183 (1998).
17. Y.H. Mohamed and V.P. Reshetnikov, *Astrofizika* 54, 181 (2011).
18. P.B. Nair and R.G. Abraham, *Astrophys. J. Suppl. Ser.* 186, 427 (2010).
19. V.P. Reshetnikov, *Astron. Lett.* 24, 153 (1998).
20. V.P. Reshetnikov, *Astron. Astrophys.* 353, 92 (2000).
21. V.P. Reshetnikov and N.Ya. Sotnikova, *Astron. Astrophys. Trans.* 20, 111 (2001).
22. M. Sawicki and G. Mallen-Ornelas, *Astron. J.* 126, 1208 (2003).
23. J.M. Schombert, J.F. Wallin, and C. Struck-Marcell, *Astron. J.* 99, 497 (1990).
24. N.Ya. Sotnikova and V.P. Reshetnikov, *Izv. RAN* 62, 1757 (1998a).
25. N.Ya. Sotnikova and V.P. Reshetnikov, *Astron. Lett.* 24, 73 (1998b).
26. V. Springel and S.D.M. White, *Mon. Not. R. Astron. Soc.* 307, 162 (1999).
27. A. Toomre and J. Toomre, *Astrophys. J.* 178, 623 (1972).
28. R.E. Williams, S. Baum, L.E. Bergeron, et al., *Astron. J.* 120, 2735 (2000).
29. C. Wolf, K. Meisenheimer, M. Kleinheinrich, et al., *Astron. Astrophys.* 421, 913 (2004).